CHAPTER

1

INTRODUCTION

INTRODUCTION

1.1 Why Polymers?

It is already well known that the use of liquid electrolytes in batteries can result in excessive volume changes especially when the conducting species and solvent jointly diffuse into the electrodes. In addition to this, some solvent materials e.g. dioxolane are volatile and are considered unsafe for large electrochemical systems. Hence the need arises for a solid electrolyte system [1,2]. The rapid development in solid electrolytes began in the early sixties after the report on Ag_3SI by Reuter and Hardell in the west and Takahashi and Yamamoto in the east [3]. Ag_3SI has a high ambient electrical conductivity of 10^{-2} S cm^{-1}.

Solid state batteries were developed and some were even commercialized [4-5] although there were still problems that have to be solved. As an example, shear stress can lead to crack propagation and subsequent loss of contact at the interface between a glassy or ceramic electrolyte and the electrode materials. In the case of cells with a silver ion (Ag^+) conductor or β-alumina electrolyte such crack propagation and loss of contact occur even for small drains in current [1].

It seems that what is needed for such battery or electrochemical cell application, in particular, would be an electrolyte with good flexing properties that could accommodate volumetric expansion arising from the low conducting discharge products which resulted from the overall cell reaction. A definite property that this flexible or plastic-like or polymer material must have in order to become a solid electrolyte is the ability to host the ions that will be injected into it and enable these ions to conduct through the material.

The first polymer observed to have the ability to solvate inorganic salts was polyethylene oxide, (PEO) [6]. By the mid-seventies, the electrical conductivity of this salt-solvating polymer has been measured [7]. The technological significance of this polymer was recognized only in 1978 when Armand [1] announced the existence of a material capable of dissolving salts to form a novel class of ionic conductors. Since then, many new complexing polymers have appeared, in the search for ion conducting polymers with higher room temperature electrical conductivity. Although the structural aspects of these polymers differ, the basic principle remains the same. A salt is dissolved in a solvating polymer matrix through direct interaction between the lone pair electrons borne by a heteroatom such as oxygen or nitrogen in the polymer and the cations of the salt. This interaction yields a conductive solid solution. Today many other examples of polymer with different atoms having lone pair electrons have been found. These include polyvinylchloride (PVC) with Cl bearing the lone pair electrons, polyethylene imine (PEI) with N as the heteroatom and polyethylene succinate (PES) with lone pair electrons at the S atom.

1.2 Criteria for Polymer Electrolytes

A set of criteria [8-9] has been laid down as a guide for the selection of polymer materials for use as electrolytes in primary and secondary batteries, electrochromic devices, modified electrodes or sensors, supercapacitors, thermoelectric generators, high vacuum electrochemistry and electrochemical switching. In general for a polymer to act as a successful host, it should possess several essential characteristics. Some of these characteristics are as follows;

a) The availability of atoms or group of atoms in the polymer that have sufficient electron donating power to form coordinate bonds with the cations of the doping salt. In other words, as Armand [1] pointed out, the polymer is able to solvate the salt, MX, through interaction between its cation, M^+ and the lone pair electrons provided by N, O, S or Cl in the polymer.

b) Segmental motion of the polymer chain can occur easily.

c) The polymer chain should be flexible to ensure effective solvation of cations and to provide favourable solvation entropy.

d) The polymer should have low cohesive energy density. A low glass transition temperature, T_g, will favour this.

Although such criteria can be a useful guidance for the selection of the polymer hosts for polymer electrolytes it should not be applied so strictly so as to limit the choice of materials to be tried and tested. This is because, although many materials satisfy these criteria, they still do not show any advantage over polyethylene oxide that can dissolve a wide range of salts particularly that of group IA in the periodic table. PEO too has its disadvantages. For example, the low T_g of PEO (~ -40°C [10]) would not allow a totally amorphous PEO-salt complex to form at room temperature unless if irradiated as reported by [11]. Furthermore, according to [11], PEO can also become more crystalline with age. In our opinion, why shouldn't a material with a high T_g (greater than room temperature) be used and tested. If such material can have an amorphous nature when complexed with a salt, then even at room temperature it will remain amorphous so long as its temperature does not exceed T_g. The material however, must be able to provide sufficient electrical conductivity needed for battery application after the addition of salt that provides the conducting ions and that of a plasticizer, if necessary. Finally, it would be appreciated that the polymer itself is non-toxic and is environmental-friendly should there be any possibility of commercializing the end product (in this work the cell or battery).

1.3 Polymer Electrolytes and Their Conductivity Values

Most of the early work carried out on polymer electrolytes concentrated on PEO. Polymers have low ionic conductivity (~ 10^{-9} S cm^{-1}), but the ionic conductivity can be increased by adding some metal salts. The addition of some plasticizers like propylene carbonate (PC), ethylene carbonate (EC) or polyethylene glycol (PEG) can also increase the ionic conductivity of the polymer electrolytes [12-14]. Other polymers that have been studied include polypropylene oxide (PPO), polyethylene imine (PEI), polyvinyl alcohol (PVA), polyvinyl chloride (PVC) etc. Some polymers and their electrical conductivity values are listed in Table 1.1.

Table 1.1: Polymer electrolytes and their conductivity values.

No.	Polymer electrolytes	Conductivity (S/cm)	References
1	PEO-$LiCF_3SO_3$	2.48×10^{-4}	15
2	PEO-LiTFSI	1.20×10^{-4}	16
3	PEO-$LiCO_4$	6.11×10^{-5}	17
4	PEI-H_3PO_4	4.13×10^{-4}	18
5	PEO-$LiBF_4$	4.72×10^{-6}	19
6	PEO-$LiMoS_2$	2.03×10^{-3}	20
7	PEO-NaI	5.21×10^{-5}	21
8	PEO-$LiClO_4$	1.58×10^{-6}	22
9	PEO-$LiC(SO_2CF_3)_2$	1.00×10^{-7}	23
10	PEO-$LiN(SO_2CF_3)_2$	5.01×10^{-5}	24
11	MEEP- $LiN(SO_2CF_3)_2$	2.00×10^{-5}	24
12	PAN-$LiClO_4$	9.12×10^{-4}	25
13	AC-$AgNO_3$	2.60×10^{-5}	26
14	AC-$LiNO_3$	2.71×10^{-4}	27
15	AC-NaI	4.90×10^{-5}	28
16	AC-Ag_2SO_4	9.20×10^{-6}	29

1.4 Conductivity Mechanism in Polymers

According to [30-32], complex impedance spectroscopy is employed in the study of the kinetics and mechanisms of electrochemical processes in the polymer electrolyte. The conductivity mechanisms of the polymer electrolyte can be predicted from its conductivity variations with temperature. From the ln σT versus $10^3/T$ graphs, one of the following five patterns of behaviour can usually be observed.

a) Vogel-Tamman-Fulcher (VTF) behaviour throughout the available thermal range.

b) Arrhenius behaviour at low temperatures and VTF behaviour at higher temperatures.

c) Arrhenius behaviour throughout the temperature range but with two different activation energies, high activation energy closer to T_g, and a smaller activation energy at higher temperatures.

d) VTF behaviour for temperatures slightly greater than T_g, but Arrhenius behaviour at higher temperatures.

e) Behaviour which is very unlike either Arrhenius or VTF at all temperatures.

The first four forms of behaviours are most common. The Arrhenius behaviour follows an activated relationship;

$$\sigma T = A_1 \exp[-B_1/RT] \qquad (1.1)$$

The VTF behaviour obeys an empirical relationship that was first derived by Vogel, Tamman and Fulcher, i.e.;

$$\sigma T = A_2 \exp[-B_2/R(T - T_o)] \qquad (1.2)$$

For polymer-salt complexes, utilizing PEO and PPO, conductivity data are generally obtained for temperatures above the glass transition temperature and the conductivity data obey the empirical VTF relationship.

Miyamoto and Shibayama [33] and Cheradame [34] has given a hybrid kind of relationship that gives better fits to the conductivity data. This equation is,

$$\sigma T = A_3 \exp\left[-\frac{B_3}{R(T - T_o)} - \frac{B_3`}{RT}\right] \qquad (1.3)$$

can be seen as a superposition of the Arrhenius and VTF equations.

The ionic conductivity of polymer-salt complexes depends on the temperature range investigated. Below the glass transition temperature, the conductivity data follow a classical Arrhenius relationship indicating that the electrical behaviour of such materials is similar to that of ionic crystals. Above the glass transition temperature, conductivity variations with temperature are greater and follow the VTF behaviour often observed in molten salts.

Two microscopic justifications for such behaviour are proposed to provide physical meanings to the parameters A_i and B_i [35]. The first is based on the point defect theory and the second is based on the free volume approach. The two types of defects mostly responsible for ion transport are the Schottky and Frenkel defects. In Schottky defects, positive and negative ions leave their normal sites as a result of thermal agitation and create vacancies. Other ions then move into these vacancies. In Frenkel defects, an ion moves to an interstitial position leaving a vacancy at its lattice. Thus the term B_1 is related to the energy of defect formation and the energy of defect migration, i.e.

$$B_1 = (\Delta H_f/2) + \Delta H_m \qquad (1.4)$$

Here the first term on the right hand side of the equation represents the energy of defect formation and the second term is the migration energy.

The free volume approach involves a cooperative mechanism of the macromolecular chains or the neighbouring atoms. The term B_2 in Eqn (1.2) is then related to the local redistribution of the mean free volume evenly distributed throughout the supercooled liquid. T_o in the same equation, is the temperature at which the entropic redistribution of the free volume disappears.

The point defect and free volume approaches differ fundamentally, but the continuous behaviour observed around the glass transition temperature seems to suggest that the two interpretations can be unified. In an attempt to unify ionic transport below and above the glass transition temperature, T_g [35-36], the defect concentration, C_+ is assumed related to the Gibb's free energy of defect formation, according to the equation

$$C_+ = C \exp(-\Delta G_f/2RT) \qquad (1.5)$$

Here,

$$\Delta G_f = \Delta H_f - T\Delta S_f \qquad (1.6)$$

is the Gibb's free energy of defect formation. The first and second terms on the right hand side of the equation are the enthalpy and the entropy of defect formation respectively. Under the influence of an electric field, the mobility of the defects is given by the Brownian movement equation,

$$U_+ = \frac{Fl^2}{6RT} \nu_o P \qquad (1.7)$$

where U_+ is the electrical mobility, l the mean distance between two cationic sites, ν_o is the attempt frequency and P is the probability of a successful displacement. F is Faraday's constant, R the universal gas constant and T the absolute temperature. At $T< T_g$, P is the probability for the interstitial cation to receive an energy greater than ΔH_m which is the energy required for the cation to jump into a neighbouring position as illustrated in Fig.1.1 (a) and (b).

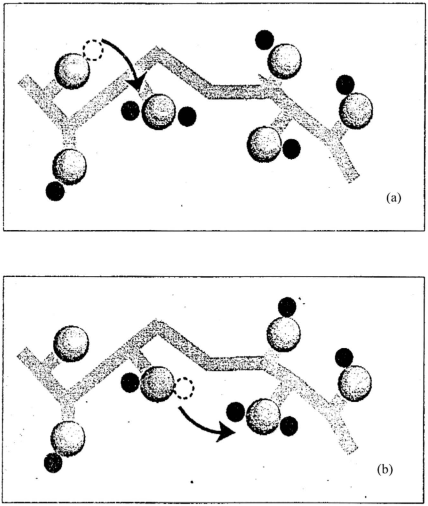

Fig.1.1(a) and (b): Cation jumping to a nearby position [35].

P is given by,

$$P = P_1 = \exp(-\Delta H_m/RT) \tag{1.8}$$

where RT is the thermal energy. At $T > T_g$, a displacement mechanism arises, Fig1.2(a) and (b).

A local deformation of the molecular chains enables the defect to be transferred to a neighbouring location. This deformation can be attributed to a local fluctuation of the free volume. The probability P_2, to locally reach the minimum free volume V_f^* needed for the defect displacement is

$$P_2 = \exp(-V_f^*/\langle V_f \rangle) \tag{1.9}$$

where $\langle V_f \rangle$ is the mean free volume and is related to $(T-T_o)$ according to

$$\langle V_f \rangle = V_o\alpha_f(T-T_o) \tag{1.10}$$

Here α_f is the thermal expansion coefficient of the free volume. Hence P_2 can be rewritten as

$$P_2 = \exp[-V_f^*/V_o\alpha_f(T-T_o)] \tag{1.11}$$

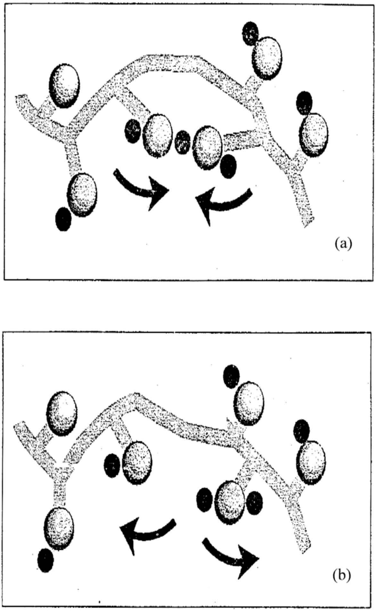

Fig.1.2(a) and (b): Segmental motion of the polymer chain leading to the transfer of charge [35].

Eqn (1.11) confirms that this second mechanism appears only above the ideal vitreous transition temperature T_o (which is usually estimated to be 50 K above T_g [8]). Above this temperature, the cationic displacement may take place either by an activated jump (P_l) or by an entropic free volume mechanism (P_2) i.e.

$$P = P_l + P_2(1-P_l) \tag{1.12}$$

implying that the second event applies to unsuccessful first events. Hence if the cationic conductivity is given by the general expression

$$\sigma_+ = FC_+U_+ \tag{1.13}$$

then upon inserting Eqn (1.5) and (1.7) into (1.13), we get

$$\sigma_+ = \frac{F^2Cl^2}{6RT} \nu_o \exp(-\Delta G_f/2RT)[P_l+P_2(1-P_l)] \tag{1.14}$$

If $P_l >> P_2$, the Eqn(1.14) becomes Eqn(1.1) with $A_l = (F^2Cl^2/R6)\nu_o\exp(\Delta S_f/2R)$ and $B_l = (\Delta H_f/2) + \Delta H_m$. If $P_l << P_2$, Eqn (1.14) simplifies to Eqn (1.3) with $A_3 = A_l$, $B_3 = RV_f^*/V_o\alpha_f$ and $B_3' = \Delta H_f/2$. Due to the exponential dependence of P_l and P_2 on T, the Arrhenius form prevails below T_g and Eqn.(1.3) prevails above T_g. Although the microscopic model considers only one charge carrier, i.e. the cation, it is also true for anionic conduction. Souquet et al [35] has illustrated this in Fig. 1.3 for a PEO-salt complex.

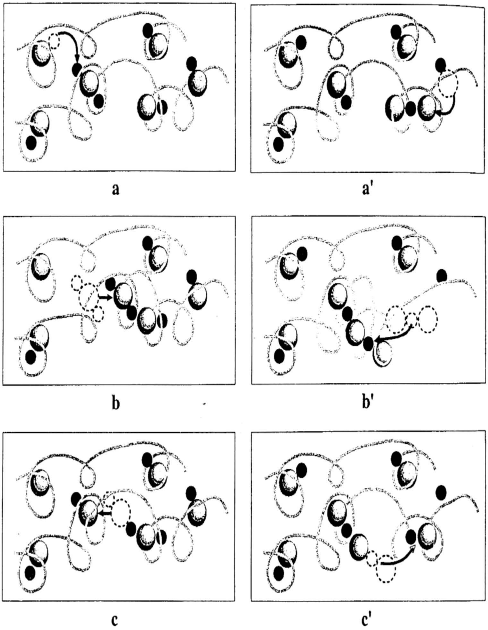

Fig.1.3: Cation conduction (a), (b) and (c). Anion conduction (a'), (b') and (c') [35].

1.5 What is Chitosan?

Fig. 1.4 (a), (b) and (c) shows the structure of chitin, cellulose and chitosan. Chitosan has an amide group (-NH_2) that makes it different from

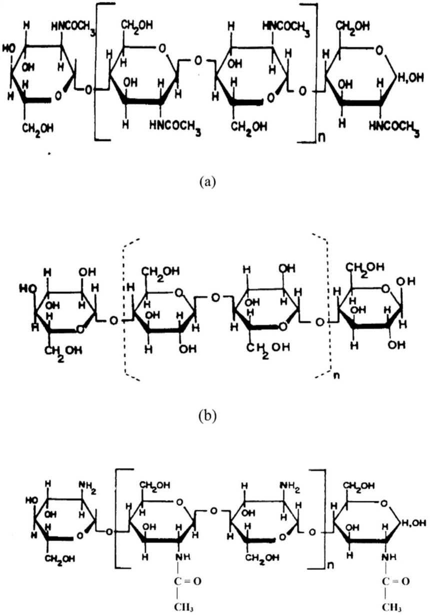

(a)

(b)

(c)

Fig. 1.4: Structure of (a) chitin (b) cellulose and (c) chitosan.

chitin or cellulose. The nitrogen atom in the amide functional group and the oxygen atom in the hydroxyl functional group each bear a lone pair electron. Chitosan can be derived from chitin. The process of chitosan derivation from chitin is called deacetylation [37-38]. According to Muzzarelli [39], during the second quarter hour of normal chitin deacytelation, the viscosity of the product decreases dramatically with time; from 5000 centipoises to ~800 centipoises. When the duration of deacetylation is long enough to allow dissolution of the product in dilute acetic acid, the product is called "chitosan" and sometimes, "deacetylated chitin". Apart from acetic acid, formic acid can also be used to dissolve chitosan.

The first observation of chitosan in living systems was in the mycelia and sporangiophores of *Phycomyces blakesleeanus* [39]. In the sixties, it was shown that chitosan comprises 32.7% of the cell wall composition of filamentous *Mucor rouxii* and 27.9% of the cell wall composition of yeast-like forms of *Mucor rouxii*. These data demonstrate that chitosan is the most abundant component of the cell wall of the two forms of *Mucor rouxii*.

1.6 General Characteristics of Chitosan

1.6.1 Film forming ability

Films or membranes are easily obtained from chitosan rather than chitin. The chitosan membrane is also the first natural polymer chelating membrane. Chitosan and chitosan acetate films do not possess any pores. They are homogeneous and have high mechanical strength [39-40].

1.6.2 Optical properties

The most significant parts of the infrared spectra of chitin and chitosan are those showing the amide bands at 1665, 1555 and 1313 wavenumbers. The band at 1665 cm^{-1} is assigned to the C=O stretching. The band at 1555 cm^{-1} is assigned to the N-H deformation in the CONH plane and the band at 1313 cm^{-1} is assigned to CN bond and CH_2 wagging.

The chitosan spectrum differs from that of chitin. In the chitosan spectrum, a band at 1590 cm^{-1} predominates over the one at 1665 cm^{-1}. From the infrared spectra, it can be observed that the amide bands will be shifted to the longer wavelengths when complexation has occurred between the amide group and the metal ions as proven by Muzzarelli et al [39,41].

1.6.3 Chelation of Metal Ions

The fact that chitosan has a lone pair electron in the amide group and can react as donor electrons to form coordinate bonds with cations has been established [39]. However, other investigations, also quoted from the same reference have demonstrated that large amounts of salt from the IA group metals; lithium, sodium, potassium, cesium and thallium do not produce any appreciable alterations on chitosan. If there is no interaction between the doping salt and the lone pair electrons of the nitrogen atom in the amide group, then the criteria for a polymer host to become a successful polymer electrolyte will be violated. Hence in this work, we have to show that by preparing the film using the solution cast technique complexation will occur between chitosan and the lithium ions.

1.6.4 Glass Transition Temperature

There are not many reports on the thermal analysis of chitosan. Muzzarelli [39] reported that chitosan undergoes degradation at high temperatures in air. Analysis have shown that chitosan cannot withstand temperatures higher than 100°C. However, Sakurai et al [42] have succeeded in observing the glass transition temperature, T_g of chitosan by thermal analysis. The T_g of chitosan was reported at 203°C.

1.7 Lithium cells

The solid state lithium cell consists of three major components as shown schematically in Fig. 1.5.

i) The anode (negative electrode) – oxidation occurs where an electron is given out to the external circuit.

$$Li \rightarrow Li^+ + e^-$$

ii) The cathode (positive electrode) - reduction occurs where electrons from the external circuit are accepted.

$$X + e^- \rightarrow X^-$$

iii) The electrolyte - the ionic conductor which provides the medium for the transfer of ions inside the cell between the anode and the cathode.

The anode is selected with the following properties; an efficient oxidizing agent, good conductivity, stability, easy to fabricate and inexpensive. Metals are mainly used as the anode material. The cathode must be an efficient reducing agent. Most of the cathode materials are metallic oxide, which are stable when in contact with the electrolyte. The electrolyte must have good ionic conductivity but it must be a weak electron conductor so as to prevent internal short-circuiting. Also the electrolyte must not react with the electrode materials.

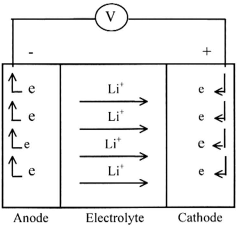

Fig. 1.5: Electrochemical operation of cell (discharge) [43]

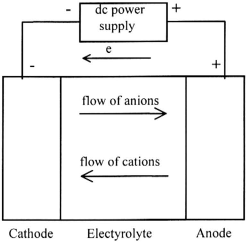

Fig. 1.6: Electrochemical operation of cell (charge) [43]

Lithium cells can be classified as primary (non-rechargeable) or secondary (rechargeable), depending on their capability of being electrically recharged. Primary cells are not capable of being recharged electrically and, hence, are disposed off once discharged. Many primary cells are termed 'dry cells'. Secondary cells can be recharged electrically, after discharge, to their original condition by passing current through them in the opposite direction to that of the discharge current as shown in Fig. 1.6.

As shown in Fig. 1.5, when the cell is connected to the external load, the cell will be discharged. Chemical reactions occur in both electrodes. At the anode (negative electrode), the discharge reaction is the oxidation of the anode material to its cation with the release of an electron.

$$M \longrightarrow M^+ + e^-$$

At the cathode (positive electrode), the cathode material is reduced to its anion with the acceptance of an electron.

$$X + e^- \longrightarrow X^-$$

When these two half-cell reactions occur, the overall cell reaction is written as below;

$$M + X \longrightarrow M^+ + X^-$$

Electrons will flow from the anode through the external load to the cathode. The electrical circuit is completed by the flow of anions and cations to the cathode and anode respectively.

Since the cell is secondary, it can be recharged. During charging, the current flow is reversed and oxidation takes place at the positive electrode and reduction at the negative electrode. The reaction at the negative electrode is;

$$M^+ + e^- \longrightarrow M$$

At the positive electrode the corresponding reaction is

$$X^- \longrightarrow X + e^-$$

and the overall reaction is as follow;

$$X^- + M^+ \longrightarrow X + M$$

After charging, a secondary cell reverts to its original chemical state and is ready to further discharge.

1.8 Some Characteristics of Lithium Cells

Cells using lithium anodes have many advantages. The advantages include high voltage, high energy density, operation over wide temperature range, good power density, have flat discharge characteristics and superior shelf life [43]. Discharging the cell by draining a constant current out of the cell will give a discharge curve as shown in Fig. 1.7.

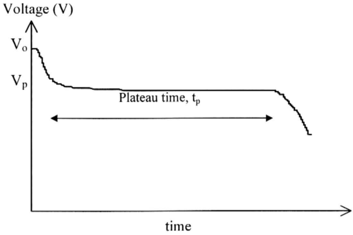

Fig. 1.7: A typical discharge characteristic.

From Fig. 1.7 some cell characteristics can be obtained:

$$\text{Current density} = \frac{\text{Current, } I}{\text{Area of electrode, } A} \ (\text{A/cm}^2)$$

$$\text{Discharge capacity} = \frac{\text{Current, } I \text{ x Plateau time, } t_p \text{ (Ah)}}{\text{Weight of the cell}} \ (\text{Ah/kg})$$

$$\text{Energy density} = \text{Plateau Voltage, } V_p \text{ x Discharge capacity (Wh/kg)}$$

$$\text{Power density} = \frac{\text{Plateau Voltage, } V_p \text{ x Current, } I}{\text{Weight of the cell}} \ (\text{W/kg})$$

Table 1.2 lists some lithium cells and their respective discharge capacity as obtained from the literature.

Table 1.2: Some characteristics of lithium cells

Cells	Discharge Capacity (mAh/g)	Ref.
$LiMnO_2/LiAl_2F_6/Li$	110	44
$LiNiO_2/LiClO_4$-PC/C	125	45
C/$LiClO_4$-PC/$LiCoO_2$	135	45
Graphite/$LiPF_4$-EC/$LiCoO_2$	370	46
Carbon fibre/$LiPF_4$-PC/$LiCoO_2$	80	46
Coke/$LiPF_4$-PC/$LiCoO_2$	180-240	46
Li/PAN-EC-PC-$LiClO_4/LiV_3O_8$	84-100	47

1.9 Objectives Of The Present Investigation

The main objective of this work is to fabricate rechargeable solid state electrochemical cells from chitosan-based polymer electrolytes complexed with lithium triflate ($LiCF_3SO_3$). To date, there is only one report [27] concerning chitosan-based cells with a lithium salt added to the chitosan-based electrolyte. Hence, in order to fabricate the cells, knowledge of the $LiCF_3SO_3$ concentration that gives the highest electrical conducting film that can fulfill the minimum conductivity requirement for electrolyte application in electrochemical cells must be obtained. Since there is no reference that can give such information to start off the work, the investigation will have to begin from scratch.

It is known [48-49] that polymers of different molecular weights will form films by the solution cast technique with different electrical conductivity values. Therefore it is important to find out whether the right type of chitosan to use is a high, medium or low molecular weight chitosan. Having determined the appropriate chitosan to use, it would be useful to study the possibility of enhancing the electrical conductivity of the chitosan film by the addition of plasticizers such as ethylene carbonate (EC) and propylene carbonate (PC). When the better plasticizer and its conductivity optimizing content is known, $LiCF_3SO_3$ will be used as the doping salt and added to the chitosan, plasticizer and acetic acid solutions during further preparation. All samples will be prepared by the solution cast technique to form a thin film.

Before the film with the highest electrical conductivity is used to fabricate electrochemical cells, all samples prepared will be characterized by X-ray diffraction (XRD) to study the effect of the dissolution of the salt on the nature of the polymer and to determine the occurrence of complexation. The occurrence of complexation is an important criterion for a polymer to be considered as an electrolyte. Characterization by Fourier Transform Infrared Spectroscopy (FTIR) and X-ray Photoelectron Spectroscopy (XPS) will also be carried out to double-check the occurrence of complexation between the salt and the polymer. The transference number for the highest electrical conductivity will be measured to determine which species of ions act as the major conductor.

The electrical conductivity of all the samples will be measured by impedance spectroscopy. Other immittance responses will be calculated from the impedance data to determine whether the materials prepared are truly ionic conductors or not. The presence or possible presence of a peak in the modulus spectra will confirm whether the material is an ionic conductor and therefore suitable for application as an electrolyte in a solid polymer electrochemical cell. Measurement of conductivity at various temperatures will be carried out to determine the mechanism of ionic conduction in the films.

The film with the highest conductivity (now known to be an ionic conductor) will be used to fabricate the cells. The charge-discharge characteristics will be measured.